Chapter 9

Critical Phenomena: Landau Theory and the Renormalization Group Method

24 May 2009

We first discuss a phenomenological mean-field theory of phase transitions due to Landau and introduce the ideas of universality and scaling near critical points. The breakdown of mean-field theory near a critical point leads us to introduce the renormalization group method, which has had a major impact on our understanding of phase transitions, quantum field theory, and turbulence. We introduce the renormalization group method in the context of percolation, a simple geometrical model that exhibits a continuous transition, and then apply renormalization group methods to the Ising model.

9.1 Landau Theory of Phase Transitions

The qualitative features of mean-field theory can be summarized by a simple phenomenological expression for the free energy due to Landau. We will introduce the Landau theory in the context of the Ising model, but the power of the Landau formulation of mean-field theory is that it can be applied to a wide variety of phase transitions ranging from superconductors to liquid crystals and first-order as well as continuous phase transitions.

One of the assumptions of the Landau theory is that a phase transition can be characterized by an *order parameter*, which we take to be the magnetization m. We choose the magnetization as the order parameter because it is zero for $T > T_c$, nonzero for $T \leq T_c$, and its behavior characterizes the nature of the transition.

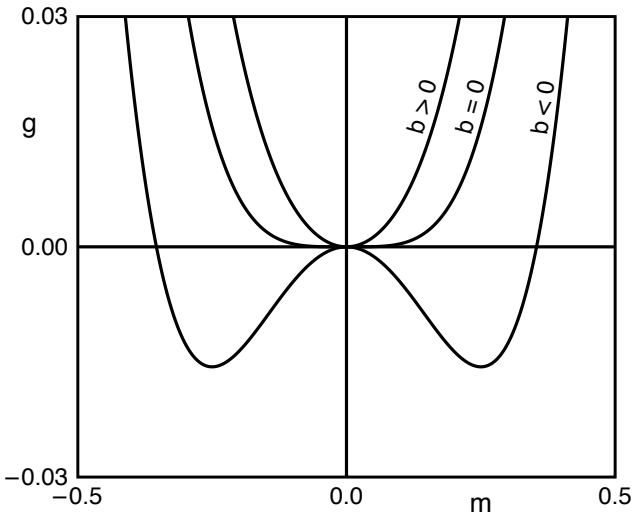

Figure 9.1: The dependence of the Landau form of the free energy density g on the order parameter m for $b = -1$, 0, and 1 with $c = 16$. The minima of g for $b = -1$ are at $m = \pm 0.250$.

Because m is small near the critical point, it is reasonable to assume that the (Gibbs) free energy density g (the free energy per unit volume) can be written in the form

$$g(T, m) = a(T) + \frac{b(T)}{2} m^2 + \frac{c(T)}{4} m^4 - Hm, \tag{9.1}$$

for a given value of H. The assumption underlying the form (9.1) is that g can be expanded in a power series in m about $m = 0$ near the critical point. Although the assumption that g is an analytic function of m turns out to be incorrect, Landau theory, like mean-field theory in general, is still a useful tool. Because $g(T, m)$ is symmetrical about $m = 0$ for $H = 0$, there are no odd terms in (9.1). The coefficients b and c are as yet unspecified. We will find that some simple assumptions for the temperature-dependence of the coefficients b and c will yield the results of mean-field theory that we found in Section 5.7.

The equilibrium value of m is the value that minimizes the free energy. In Figure 9.1 we show the dependence of g on m for $H = 0$. We see that if $b > 0$ and $c > 0$, then the minimum of g is at $m = 0$, corresponding to the high temperature phase. If $b < 0$ and $c > 0$, then the minimum of g is at $m \neq 0$, corresponding to the low temperature ferromagnetic phase. To find the minimum of g we take the derivative of g with respect to m and write for $H = 0$

$$\frac{\partial g}{\partial m} = bm + cm^3 = 0. \tag{9.2}$$

One obvious solution of (9.2) is $m = 0$, which mimimizes g for $b > 0$ and $c > 0$. The nonzero solution of (9.2) is $m^2 = -b/c$. If we make the simple assumption that $b = b_0(T - T_c)$ and $c > 0$, we find

$$m = \pm \Big(\frac{b_0}{c}\Big)^{1/2} (T_c - T)^{1/2} = \pm \Big(\frac{b_0 T_c}{c}\Big) \epsilon^{1/2}, \qquad (T \leq T_c) \tag{9.3}$$

where the dimensionless parameter ϵ is a measure of the deviation from the critical temperature:

$$\epsilon = \frac{|T_c - T|}{T_c}. \tag{9.4}$$

Equation (9.3) predicts that the critical exponent $\beta = 1/2$. Compare this result for β to what we found from the mean-field theory treatment of the Ising model on page 260. How does this value of β compare to the exact value of β for the two-dimensional Ising model?

The behavior of the specific heat C can be found from the relation $C = T\partial s/\partial T$. The entropy density is given by

$$s = -\frac{\partial g}{\partial T} = -a' - \frac{b'}{2}m^2 - \frac{b}{2}(m^2)' - \frac{c}{4}(m^4)', \tag{9.5}$$

where the primes in (9.5) denote the derivative with respect to T, and we have assumed that c is independent of T. From (9.5) and our assumed for $b(T)$ we have

$$C = T\frac{ds}{dT} = -Ta'' - Tb'(m^2)' - \frac{cT}{4}(m^4)''. \tag{9.6}$$

Because $m = 0$ for $T \geq T_c$, we have $C \to -Ta''$ as $T \to T_c^+$. For $T \to T_c^-$ we have $(m^2)' = -b_0/c$, $b' = b_0$, and $(m^4)'' \to 2(b_0/c)^2$. Hence, we obtain

$$C = \begin{cases} -Ta'' & (T \to T_c^+) \\ -Ta'' + \dfrac{Tb_0^2}{2c}. & (T \to T_c^-) \end{cases} \tag{9.7}$$

We see that Landau theory predicts a jump in the specific heat at the critical point, just as we previously obtained in our mean-field theory treatment of the Ising model in Section 5.7.

Problem 9.1. Predictions of the Landau theory for the critical exponents γ and δ

(a) Show that the solution of $bm+cm^3-H = 0$ minimizes g for $H \neq 0$, and hence $\chi^{-1} = (b+3cm^2)$. Then show that $\chi^{-1} = b = b_0(T - T_c)$ for $T > T_c$ and $\chi^{-1} = 2b_0(T_c - T)$ for $T < T_c$. Hence Landau theory predicts the same power law form for χ above and below T_c with $\gamma = 1$.

(b) Show that $cm^3 = H$ at the critical point, and hence $\delta = 3$, where δ is defined by $m \sim H^{1/\delta}$. □

We can generalize Landau theory to incorporate spatial fluctuations by writing

$$g(\mathbf{r}) = a + \frac{b}{2}m^2(\mathbf{r}) + \frac{c}{4}m^4(\mathbf{r}) + \frac{\lambda}{2}[\nabla m(\mathbf{r})]^2 - m(\mathbf{r})H, \tag{9.8}$$

where the parameter $\lambda > 0$. The gradient term in (9.8) expresses the fact that the free energy is increased by spatial fluctuations in the order parameter. The form of the free energy density in (9.8) is commonly known as the *Landau-Ginzburg* form. The total free energy is given by

$$G = \int g(\mathbf{r})\, d\mathbf{r}, \tag{9.9}$$

and the total magnetization is

$$M = \int m(\mathbf{r})\, d\mathbf{r}. \tag{9.10}$$

We follow the same procedure as before and minimize the total free energy:

$$\delta G = \int \Big[\delta m(\mathbf{r})[b\, m(\mathbf{r}) + c\, m^3(\mathbf{r}) - H] + \lambda \nabla \delta m(\mathbf{r}) \cdot \nabla m(\mathbf{r})\Big] d\mathbf{r} = 0. \tag{9.11}$$

The last term in the integrand of (9.11) can be simplified by integrating by parts and requiring that $\delta m(\mathbf{r}) = 0$ at the surface. In this way we obtain

$$b\, m(\mathbf{r}) + c\, m(\mathbf{r})^3 - \lambda \nabla^2 m(\mathbf{r}) = H(\mathbf{r}). \tag{9.12}$$

Equation (9.12) reduces to the usual Landau theory by letting $H(\mathbf{r}) = H$ and $\nabla m(\mathbf{r}) = 0$.

To probe the response of the system we apply a localized magnetic field $H(\mathbf{r}) = H_0 \delta(\mathbf{r})$ and write

$$m(\mathbf{r}) = m_0 + \phi(\mathbf{r}), \tag{9.13}$$

We assume that the spatially varying term $\phi(\mathbf{r})$ is small so that $m(\mathbf{r})^3 \approx m_0^3 + 3m_0^2 \phi(\mathbf{r})$. We then substitute (9.13) into (9.12) and obtain

$$\nabla^2 \phi(\mathbf{r}) - \frac{b}{\lambda}\phi(\mathbf{r}) - 3\frac{c}{\lambda} m_0^2\, \phi(\mathbf{r}) - \frac{b}{\lambda} m_0 - \frac{c}{\lambda} m_0^3 = -\frac{H_0}{\lambda}\delta(\mathbf{r}). \tag{9.14}$$

If we substitute $m_0 = 0$ for $T > T_c$ and $m_0^2 = -b/c$ for $T < T_c$ into (9.14), we obtain

$$\nabla^2 \phi - \frac{b}{\lambda}\phi = -\frac{H_0}{\lambda}\delta(\mathbf{r}) \qquad (T > T_c) \tag{9.15a}$$

$$\nabla^2 \phi + 2\frac{b}{\lambda}\phi = -\frac{H_0}{\lambda}\delta(\mathbf{r}). \qquad (T < T_c) \tag{9.15b}$$

Note that $\phi(\mathbf{r})$ in (9.15) satisfies an equation of the same form as we found in the Debye-Hučkel theory (see Section 8.8, page 422).

The easiest way of solving equations of the form,

$$\left[\nabla^2 - \xi^{-2}\right]\phi(\mathbf{r}) = -4\pi A \delta(\mathbf{r}), \tag{9.16}$$

is to transform to k-space and write (for three dimensions)

$$\phi(\mathbf{r}) = \int \frac{d^3k}{(2\pi)^3} e^{-i\mathbf{k}\cdot\mathbf{r}} \phi(\mathbf{k}). \tag{9.17}$$

We then write

$$\nabla^2 \phi(\mathbf{r}) = -\int \frac{d^3k}{(2\pi)^3} k^2 e^{-\mathbf{k}\cdot\mathbf{r}} \phi(\mathbf{k}), \tag{9.18}$$

and the Fourier transform of (9.16) becomes

$$[k^2 + \xi^{-2}]\phi(\mathbf{k}) = 4\pi A, \tag{9.19}$$

or

$$\phi(\mathbf{k}) = \frac{4\pi A}{k^2 + \xi^{-2}}. \tag{9.20}$$

The inverse Fourier transform of (9.20) gives

$$\phi(\mathbf{r}) = \int \frac{d^3k}{(2\pi)^3} \frac{4\pi A}{k^2 + \xi^{-2}} e^{-i\mathbf{k}\cdot\mathbf{r}} = \frac{A}{r} e^{-r/\xi}. \tag{9.21}$$

Hence we see that the solution of (9.15) can be written as

$$\phi(r) = \frac{H_0}{4\pi\lambda} \frac{1}{r} e^{-r/\xi}, \tag{9.22}$$

with

$$\xi(T) = \begin{cases} \left[\dfrac{\lambda}{b(T)}\right]^{1/2} & (T > T_c) \\ \left[\dfrac{-\lambda}{2b(T)}\right]^{1/2} & (T < T_c) \end{cases} \tag{9.23}$$

Thus, ϕ is a quantitative measure of the response to a small magnetic field applied at a single point. Because $\phi(r)$ is proportional to H, it is an example of a linear response, and its positive sign indicates that the system is paramagnetic. The exponential form for $\phi(r)$ indicates that this response decays rapidly as the distance from the applied field ranges beyond ξ. As we will see, ξ plays another important role as well, namely it can be interpreted as the *correlation length*. Because $b(T) = b_0(T - T_c)$, we see that ξ diverges both above and below T_c as

$$\xi(T) \sim \epsilon^{-\nu}, \tag{9.24}$$

with $\nu = 1/2$.

Problem 9.2. Solution of (9.16)
Work out the steps that were skipped in obtaining the solution (9.21) of (9.16).

The large value of ξ near T_c implies that the fluctuations of the magnetization are correlated over large distances. We can understand how the fluctuations are correlated by calculating the correlation function

$$G(r) = \langle m(r)m(0)\rangle - \langle m\rangle^2. \tag{9.25}$$

(Do not confuse $G(r)$ with the free energy G.) As in Chapter 8 we will write thermal averages as $\langle \ldots \rangle$. We can relate $G(r)$ to the first-order response $\phi(r)$ by the following considerations (see page 234). We write the total energy in the form

$$E = E_0 - \int m(\mathbf{r})H(\mathbf{r})\, d\mathbf{r}, \tag{9.26}$$

where E_0 is the part of the total energy E that is independent of $H(\mathbf{r})$. We have

$$\langle m(\mathbf{r})\rangle = \frac{\sum_s m_s(\mathbf{r})\, e^{-\beta[E_{0,s} - \int m_s(\mathbf{r}')H(\mathbf{r}')\, d\mathbf{r}']}}{\sum_s e^{-\beta[E_{0,s} - \int m_s(\mathbf{r}')H(\mathbf{r}')\, d\mathbf{r}']}}, \tag{9.27}$$

where $E_{0,s}$ and $m_s(\mathbf{r})$ denote the values of E_0 and $m(\mathbf{r})$ in microstate s. We see that

$$\frac{\delta\langle m(\mathbf{r})\rangle}{\delta H(0)} = \beta\big[\langle m(\mathbf{r})m(0)\rangle - \langle m(\mathbf{r})\rangle\langle m(0)\rangle\big] = \beta G(\mathbf{r}). \tag{9.28}$$

Because $m(\mathbf{r}) = m_0 + \phi(\mathbf{r})$, we also have $\delta\langle m(\mathbf{r})\rangle/\delta H(0) = \phi(\mathbf{r})/H_0$ so that from (9.28) we obtain $G(r) = kT\phi(\mathbf{r})/H_0$. We substitute $\phi(\mathbf{r})$ from (9.22) and find that

$$G(r) = \frac{kT}{4\pi\lambda}\frac{1}{r}e^{-r/\xi}. \tag{9.29}$$

From the form of (9.29) we recognize ξ as the correlation length in the neighborhood of T_c, and we see that the fluctuations of the magnetization are correlated over increasingly large distances as the system approaches the critical point.

At $T = T_c$, $\xi = \infty$, and $G(r) \sim 1/r$. For arbitrary spatial dimension d we can write the r-dependence of $G(r)$ at $T = T_c$ as

$$G(r) \sim \frac{1}{r^{d-2+\eta}}, \qquad (T = T_c) \tag{9.30}$$

where we have introduced another critical exponent η. We see that Landau-Ginzburg theory yields $\eta = 0$ in three dimensions. It can be shown that Landau-Ginzburg theory predicts $\eta = 0$ in all dimensions.

Problem 9.3. Relation of the linear response to the spin-spin correlation function

Derive the relation (9.28) between the linear response $\delta\langle m(\mathbf{r})\rangle/\delta H(0)$ and the spin correlation function $G(r)$. □

The existence of long-range correlations of the order parameter is associated with the divergence of the susceptibility χ. As we showed in Chapter 5, χ is related to the fluctuations in M (see (5.17)):

$$\chi = \frac{1}{NkT}\big[\langle M^2\rangle - \langle M\rangle^2\big] = \frac{1}{NkT}\big\langle\big[M - \langle M\rangle\big]^2\big\rangle. \tag{9.31}$$

We write

$$M - \langle M\rangle = \sum_{i=1}^{N}[s_i - \langle s_i\rangle], \tag{9.32}$$

and

$$\chi = \frac{1}{NkT}\sum_{i,j=1}^{N}[\langle s_i s_j\rangle - \langle s_i\rangle\langle s_j\rangle] = \frac{1}{kT}\sum_{j=1}^{N}G_{1j}, \tag{9.33}$$

where $G_{ij} = \langle s_i s_j\rangle - \langle s_i\rangle\langle s_j\rangle$. We have used the definition of G_{ij} and the fact that all sites are equivalent. The generalization of (9.33) to a continuous system is

$$\chi = \frac{1}{kT}\int G(r)\,d\mathbf{r}. \tag{9.34}$$

Problem 9.4. The divergence of the susceptibility and long-range correlations

Show that the relation (9.34) and the form (9.29) of $G(r)$ implies that $\chi \sim |T - T_c|^{-1}$. Hence, the divergence of the susceptibility is associated with the existence of long-range correlations. □

Range of Validity of Mean-Field Theory. As discussed briefly in Section 5.7, mean-field theory must break down when the system is sufficiently close to a critical point. That is, mean-field theory is applicable only if the fluctuations in the order parameter are much smaller than their mean value. Conversely, if the relative fluctuations are large, mean-field theory must break down. One criterion for the validity of mean-field theory can be expressed as

$$\frac{\int [\langle m(\mathbf{r})m(0)\rangle - \langle m(\mathbf{r})\rangle\langle m(0)\rangle]\, d\mathbf{r}}{\int m^2\, d\mathbf{r}} \ll 1. \tag{9.35}$$

The condition (9.35) is known as the *Ginzburg criterion* and gives a criterion for the self-consistency of mean-field theory. If we substitute $G(r)$ from (9.29) into (9.35) and integrate over a sphere of radius ξ, we find

$$\frac{kT}{4\pi\lambda}\int_0^\xi \frac{e^{-r/\xi}}{r}\, 4\pi r^2 dr = \frac{kT\xi^2}{\lambda}\Big(1 - \frac{2}{e}\Big) \approx \frac{0.264kT\xi^2}{\lambda}. \tag{9.36}$$

Hence, the Ginzburg criterion for the validity of mean-field theory becomes

$$\frac{0.264kT\xi^2}{\lambda} \ll \frac{4\pi}{3}\xi^3 m^2, \tag{9.37}$$

or

$$\frac{0.063}{\lambda} \ll \xi m^2. \qquad \text{(Ginzburg criterion)} \tag{9.38}$$

The numerical factors in (9.36)–(9.38) should not be taken seriously.

Because $\xi \sim |T - T_c|^{-1/2}$ and $m^2 \sim (T - T_c)$, we see that the product ξm^2 approaches zero as $T \to T_c$ and the Ginzburg criterion will not be satisfied for T sufficiently close to T_c. Hence, mean-field theory must break down when the system is sufficiently close to a critical point. However, there exist some systems, for example, conventional superconductivity, for which the correlation length is very large even far from T_c and (9.38) is satisfied in practice for ϵ as small as $\sim 10^{-14}$. For liquid ^{4}He mean-field theory is applicable for $\epsilon \sim 0.3$.[1]

Problem 9.5. The Ginzburg criterion in terms of measurable quantities

The Ginzburg criterion can be expressed in terms of the measurable quantities T_c, ξ_0, the correlation length at $T = 0$, and the jump in the specific heat ΔC at $T = T_c$.

(a) Use (9.23) and the relation $b = b_0(T - T_c)$ to express the correlation length as

$$\xi(T) = \xi_0 \epsilon^{-1/2}, \tag{9.39}$$

[1] A system such as the Ising model will exhibit mean-field behavior in the limit of infinite range interactions (see Section 5.10.5). If the interaction range is long but finite, the system will exhibit mean-field behavior near but not too near the critical point, and then *crossover* to non-mean-field behavior close to the critical point. See for example, Erik Luijten, Henk W. J. Blöte, and Kurt Binder, "Medium-range interactions and crossover to classical critical behavior," Phys. Rev. **54**, 4626–4636 (1996).

where ξ_0 is the correlation length extrapolated to $T = 0$. Show that that ξ_0 is given by

$$\xi_0^2 = \frac{\lambda}{2b_0 T_c}. \tag{9.40}$$

Hence we can eliminate the parameter λ in (9.38) in favor of the measurable quantity ξ_0 and the parameter b_0.

(b) Express b_0 in terms of the jump ΔC in the specific heat at T_c by using (9.7) and show that $b_0^2 = (2c/T_c)\Delta C$.

(c) Use the relation (9.3) for $m(T)$ in (9.38), and show that the Ginzburg criterion can be expressed as

$$\frac{0.016}{\xi_0^3\, T_c\, \Delta C} \ll |\epsilon|^{1/2}. \tag{9.41}$$

Note that if ξ_0 is large as it is for conventional superconductors ($\xi_0 \sim 10^{-7}$ m), then the Ginzburg criterion is satisfied for small values of ϵ. □

Problem 9.6. Generalization of Ginzburg criterion to arbitrary dimension

The general solution for the correlation function $G(r)$ in arbitrary spatial dimension d is not as simple as (9.29), but for $r \gg 1$ has the form

$$G(r) \sim \frac{e^{-r/\xi}}{r^{d-2}}. \tag{9.42}$$

Generalize the Ginzburg criterion (9.35) to arbitrary d and show that it is satisfied if $d\nu - 2\beta - 2\nu$, or

$$d > 2 + 2\beta/\nu. \tag{9.43}$$

Ignore all numerical factors. □

Because mean-field theory yields $\beta = 1/2$ and $\nu = 1/2$, we conclude from Problem 9.6 and the condition (9.43) that the Ising model will exhibit mean-field behavior for T near T_c if $d > d_c = 4$. At $d = d_c$ the *upper critical dimension*, there are logarithmic corrections to the mean-field critical exponents. That is, near the critical point, the exponents predicted by mean-field theory are exact for dimensions greater than four.[2]

9.2 Universality and Scaling Relations

From our simulations of the Ising model and our discussions of mean-field theory near the critical point we have learned that critical phenomena are characterized by power law behavior and critical exponents. This behavior is associated with the divergence of the correlation length as the critical

[2]It is possible to calculate the critical exponents in less than four dimensions by an expansion in the small parameter $d - 4$ with Landau theory as the zeroth order term. The seminal paper is by Kenneth G. Wilson and Michael E. Fisher, "Critical exponents in 3.99 dimensions," Phys. Rev. Lett. **28**, 240–243 (1972). (A strong background in field theory is needed to understand this paper.)

Fisher	$\gamma = \nu(2 - \eta)$
Rushbrooke	$\alpha + 2\beta + \gamma = 2$
Widom	$\gamma = \beta(\delta - 1)$
Josephson	$\nu d = 2 - \alpha$

Table 9.1: Examples of scaling relations between the critical exponents.

point is approached. We also found an example of universality. That is, mean-field theory predicts that the critical exponents are independent of dimension and are the same for the Ising model and the gas-liquid critical points (see page 380). Because the critical exponents of the Ising model depend on dimension, we know that this statement of universality is too strong. Nonetheless, we will find that some aspects of the universality predicted by mean-field theory are correct.

Aside from the intrinsic importance and occurrence of critical phenomena in nature, an understanding of critical phenomena can serve as an introduction to several important ideas in contemporary physics. These ideas are important in a wide range of areas including condensed matter physics, particle physics, plasma physics, and turbulence. In this section we will discuss two of these ideas – universality and scaling. The renormalization group method, which provides a framework for understanding the origins of both universality and scaling, will be introduced in Sections 9.4–9.6. A discussion of a related method, conformal invariance, is beyond the scope of the text.

To better appreciate the application of universality, recall the nature of the Heisenberg model introduced in Section 5.10.1. In this model each spin has three components S_x, S_y, and S_z, and the order parameter is a three-dimensional vector. We say that the Heisenberg model corresponds to $n = 3$, where n is the number of components of the order parameter. If the spins are restricted to be in a plane, then the model is called the XY (or planar) model and $n = 2$. The now familiar Ising model corresponds to $n = 1$.

The superfluid and (conventional) superconducting phase transitions can be modeled by the XY model near a critical point because the order parameter is described by a quantum mechanical wave function which is characterized by an amplitude and a phase. Thus these systems correspond to $n = 2$. As we discussed in Section 5.9 and Chapter 7, the order parameter of the liquid-gas transition is a scalar and hence $n = 1$.

The assumption of universality is that the behavior of a wide variety of systems near a continuous phase transition depends only on the spatial dimension of the lattice d and the symmetry properties of the order parameter, and does not depend on the details of the interactions. The most common *universality classes* correspond to the scalar, planar, and three-dimensional vector order parameter for which $n = 1$, $n = 2$, and $n = 3$, respectively, and to the spatial dimension d. That is, the critical exponents depend on the combination (n, d). One remarkable implication of universality is that the critical exponents for the gas-liquid critical point are the same as the Ising model, even though these systems seem qualitatively different. That is, the Ising model, which is defined on a lattice, and gases and liquids look the same near their critical points if we consider long length scales. Examples of $n = 2$ are XY ferromagnets (see Problem 9.25), superfluid ^{4}He, and conventional superconductivity. The case $n = 3$ corresponds to the Heisenberg model.

The definitions of the critical exponents are summarized in Table 5.1 (see page 255). We will find in the following that only two of the six critical exponents are independent. The exponents

are related by *scaling relations* which are summarized in Table 9.1. The scaling relations are a consequence of the essential physics near the critical point; that is, the correlation length ξ is the only characteristic length of the system.

A simple way to obtain the scaling relations in Table 9.1 is to use dimensional analysis and assume that a quantity that has dimension L^{-p} is proportional to ξ^{-p} near the critical point. Because the quantity βF is dimensionless and proportional to N, we see that $\beta F/V$ has dimensions

$$[\beta f] = L^{-d}. \tag{9.44}$$

Similarly the correlation function $G(r)$ depends on L according to

$$[G(r)] = L^{2-d-\eta}. \tag{9.45}$$

From its definition in (9.25) we see that $G(r)$ has the same dimension as m^2, and hence

$$[m] = L^{(2-d-\eta)/2}. \tag{9.46}$$

If we use the relation (9.31) between χ and the variance of the magnetization, we have

$$[kT\chi] = L^{2-\eta}. \tag{9.47}$$

Finally, because $M = -\partial F/\partial H$ (see (5.16)), we have

$$[H/kT] - L^{(2+d-\eta)/2}. \tag{9.48}$$

Problem 9.7. The scaling relations

We can obtain the scaling relations by replacing L in (9.44)–(9.48) by ξ and letting $\xi \sim \epsilon^{-\nu}$.

(a) Because the dimensions of the heat capacity are the same as βf in (9.44), show that $2-\alpha = d\nu$.

(b) Use dimensional analysis to obtain the relations $-\nu(2-d-\eta)/2 = \beta$, $-\nu(2-\eta) = -\gamma$, and $\nu(2+d-\eta)/2 = \beta\delta$. Then do some simple algebra to derive the Rushbrooke and Widom scaling relations in Table 9.1. □

9.3 A Geometrical Phase Transition

Before we consider theoretical techniques more sophisticated than mean-field theory, it is instructive to first introduce a model that is simpler than the Ising model and that exhibits a continuous phase transition. This simple geometrical model, known as *percolation*, does not involve the temperature or the evaluation of a partition function and is easy to simulate. The questions that are raised by considering the percolation transition will prepare us for a deeper understanding of phase transitions in more complex systems such as the Ising model. Some of the applications of percolation include the flow of oil through porous rock, the behavior of a random resistor network, and the spread of a forest fire.

The simplest percolation model is formulated on a lattice. Assume that every lattice site can be in one of two states, "occupied" or "empty." Each site is occupied independently of its

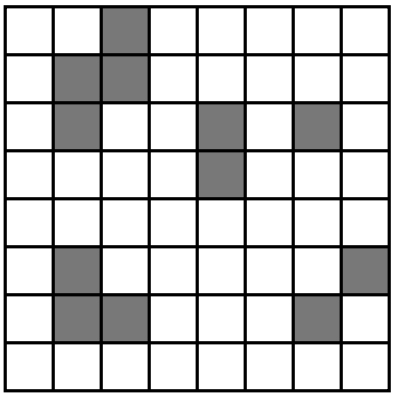

Figure 9.2: Examples of (site) percolation clusters on a square lattice for which each site has four nearest neighbors. Shown are three clusters with one site, one cluster with two sites, one cluster of three sites, and one cluster of four sites.

neighbors with probability p. This model of percolation is called *site* percolation. The nature of percolation is related to the properties of the *clusters* of occupied sites. Two occupied sites belong to the same cluster if they are linked by a path of nearest-neighbor bonds joining occupied sites (see Figure 9.2).

We can use the random number generator on a calculator to generate a random number for each lattice site. A site is occupied if its random number is less than p. Because each site is independent, the order that the sites are visited is irrelevant. If p is small, there are many small clusters (see Figure 9.3(a)). As p is increased, the size of the clusters increases. If $p \sim 1$, most of the occupied sites form one large cluster that extends from one end of the lattice to the other (see Figure 9.3(c)). Such a cluster is said to "span" the lattice and is called a *spanning* cluster. What happens for intermediate values of p, for example between $p = 0.5$ and $p = 0.7$ (see Figure 9.3(b))? It has been shown that in the limit of an infinite lattice there exists a well defined threshold probability p_c such that

For $p \geq p_c$, one spanning cluster or path exists.

For $p \leq p_c$, no spanning cluster exists and all clusters are finite.

The essential characteristic of percolation is *connectedness*. The connectedness of the occupied sites exhibits a qualitative change at $p = p_c$ from a state with no spanning cluster to a state with one spanning cluster. This transition is an example of a continuous *geometrical phase transition.* From our discussions of continuous phase transitions we know that it is convenient to define an order parameter that vanishes for $p < p_c$ and is nonzero for $p \geq p_c$. A convenient choice of the order parameter for percolation is P_∞, the probability that an occupied site is part of the spanning cluster. We can estimate P_∞ for a given configuration on a finite sized lattice from its definition:

$$P_\infty = \frac{\text{number of sites in the spanning cluster}}{\text{total number of occupied sites}}. \tag{9.49}$$

To calculate P_∞ we need to average over all possible configurations for a given value of p.

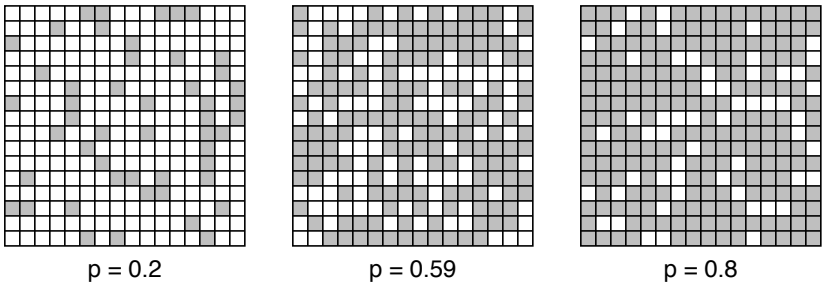

Figure 9.3: Examples of site percolation configurations for $p < p_c$, $p \approx p_c$, and $p > p_c$. The configuration at $p = 0.59$ has a spanning cluster. Find the spanning path for this configuration.

For $p < p_c$ on an infinite lattice there is no spanning cluster and $P_\infty = 0$.[3] At $p = 1$, P_∞ has its maximum value of one because only the spanning cluster exists. These properties suggest that P_∞ is a reasonable choice for the order parameter.

Problem 9.8. Estimation of P_∞

Estimate the value of P_∞ for the configuration shown in Figure 9.3(b). Accurate estimates of P_∞ require averages over many configurations. □

The behavior of P_∞ as a function of p for a finite lattice is shown in Figure 9.4. The phase transition at p_c is continuous. In the critical region near and above p_c we assume that P_∞ vanishes as

$$P_\infty \sim (p - p_c)^\beta, \tag{9.50}$$

where β denotes the critical exponent for the behavior of the order parameter neat the critical point.

Information about the clusters is given by the cluster size distribution $n_s(p)$, which is defined as

$$n_s(p) = \frac{\text{mean number of clusters of size } s}{\text{total number of lattice sites}}. \tag{9.51}$$

For $p \geq p_c$ the spanning cluster is excluded from n_s. To get an idea of how to calculate n_s, we consider $n_s(p)$ for small s on the square lattice. The probability of finding a single isolated occupied site is

$$n_1(p) = p(1 - p)^4, \tag{9.52}$$

because the probability that one site is occupied is p and the probability that all of its four neighboring sites are empty is $(1 - p)^4$. Similarly, $n_2(p)$ is given by

$$n_2(p) = 2p^2(1 - p)^6. \tag{9.53}$$

The factor of two in (9.53) is due to the two possible orientations of the two occupied sites.[4]

[3] There are configurations that span a lattice for $p < p_c$, such as a column of occupied sites, but these configurations have a low probability of occurring in the limit of an infinite lattice and may be ignored.

[4] It might be thought that there should be a factor of four on the right-hand side of (9.53) because each site has four nearest neighbors, and thus there are four ways of choosing two sites. However, because we are averaging over the entire lattice, two of these ways are equivalent.

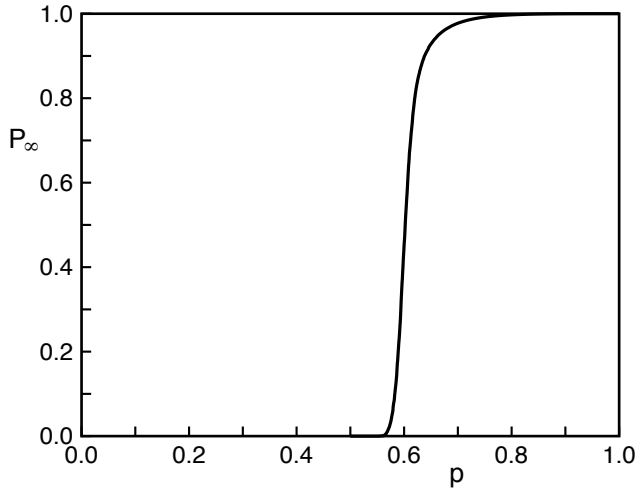

Figure 9.4: Plot of the estimated p-dependence of the order parameter P_∞ obtained by averaging over many configurations on a 128×128 square lattice.

At $p = p_c$, n_s scales with s as

$$n_s \sim s^{-\tau}. \tag{9.54}$$

A consequence of the power law relation (9.54) is that clusters of all sizes exist on an infinite lattice for $p = p_c$ (see page 255 for a similar discussion of the Ising critical point).

Many of the properties of interest are related to moments of n_s. Because Nsn_s is the number of occupied sites in clusters of size s, the quantity

$$w_s = \frac{sn_s}{\sum_s sn_s}, \tag{9.55}$$

is the probability that an occupied site chosen at random is part of an s-site cluster. The mean number of occupied sites in a (finite) cluster is defined as

$$S(p) = \sum_s sw_s = \frac{\sum_s s^2 n_s}{\sum_s sn_s}. \tag{9.56}$$

The sum in (9.56) is over the finite clusters. The quantity $S(p)$ behaves near p_c as

$$S(p) \sim (p - p_c)^{-\gamma}. \tag{9.57}$$

We can associate a characteristic length ξ with the clusters. One way is to introduce the radius of gyration R_s of a single cluster of s sites:

$$R_s{}^2 = \frac{1}{s}\sum_{i=1}^{s}(\mathbf{r}_i - \overline{\mathbf{r}})^2, \tag{9.58}$$

where

quantity	functional form	exponent	$d = 2$	$d = 3$
order parameter	$P_\infty \sim (p - p_c)^\beta$	β	5/36	0.42
mean size of finite clusters	$S(p) \sim \lvert p - p_c\rvert^{-\gamma}$	γ	43/18	1.82
connectedness length	$\xi(p) = \lvert p - p_c\rvert^{-\nu}$	ν	4/3	0.89
cluster distribution (at $p = p_c$)	$n_s \sim s^{-\tau}$	τ	187/91	2.19

Table 9.2: The critical exponents associated with the percolation transition. The exponents are known exactly in $d = 2$ on the basis of conformal theory arguments and the equivalence of percolation to the q-state Potts model (see page 269) in the limit $q \to 1$. The values of the exponents depend only on the spatial dimension and not on the symmetry of the lattice.

$$\overline{\mathbf{r}} = \frac{1}{s}\sum_{i=1}^{s} \mathbf{r}_i, \tag{9.59}$$

and $\mathbf{r}_i$ is the position of the ith site in the cluster. The statistical weight of the clusters of size s is the probability w_s that a site is a member of a cluster of size s times the number of sites s in the cluster. The *connectedness length* ξ can be defined as a weighted average over the radius of gyration of all finite clusters

$$\xi^2 = \frac{\sum_s s^2 n_s {R_s}^2}{\sum_s s^2 n_s}. \tag{9.60}$$

The connectedness length in percolation problems plays the same role as the correlation length in thermal systems. Near p_c we assume that ξ diverges as

$$\xi \sim |p_c - p|^{-\nu}. \tag{9.61}$$

Problem 9.9. Simulation of percolation

Program `Percolation` generates percolation configurations on the square lattice. The program computes $P_\infty(p)$, the fraction of states in the spanning cluster; $S(p)$, the mean number of sites in the finite clusters; $P_{\rm span}(p)$, the probability of a spanning cluster; and n_s, the number of clusters with s sites for various values of p. The clusters are shown at the default value of $p = 0.5927$, and the largest cluster is shown in red.

(a) Run the program and look at the configurations. A spanning cluster is defined as one that connects the top and bottom of the lattice and the left and right boundaries. (An alternative would be to use toroidal boundary conditions.) How would you describe the structure of the spanning clusters at $p = 0.8$? Are the clusters compact with few holes or ramified and stringy?

(b) Visually inspect the configurations at $p = p_c \approx 0.5927$. How would you describe the spanning clusters at the percolation threshold? Increase the size of the lattice. Do the spanning clusters become less dense? Note that there are clusters of all sizes at $p = p_c$.

(c) Run the program for at least 100 trials and look at the log-log plot of the cluster size distribution n_s versus s at $p = p_c$. Do you see linear behavior for some range of values of s? What functional form does this linear dependence suggest? Choose `Data Table` under the `Views` menu and fit your data to the form $n_s = As^{-\tau}$, where A and τ are fitting parameters. The exact result for τ in $d = 2$ is given in Table 9.2. How does your estimate for τ compare?

lattice	d	q	p_c (site)
linear chain	1	2	1
square	2	4	0.592746
hexagonal	2	6	1/2
simple cubic	3	6	0.3116
bcc	3	8	0.2459
fcc	3	12	0.1992

Table 9.3: Values of the percolation threshold p_c in two and three dimensions for several lattices. The value of p_c depends on the dimension d and the symmetry of the lattice. Errors in the numerical results are in the last digit. The results are taken from R. M. Ziff and M. E. J. Newman, "Convergence of threshold estimates for two-dimensional percolation," Phys. Rev. E **66**, 016129-1–10 (2002) and Chai-Yu Lin and Chin-Kun Hu, "Universal fnite-size scaling functions for percolation on three-dimensional lattices," Phys. Rev. E **58**, 1521–1527 (1998).

(d) Choose $p = 0.4$ and 0.8 and look at the log-log plots of the cluster size distribution n_s versus s. Is the qualitative behavior of n_s for large s the same as it is at $p = p_c$?

(e) *Choose L = 128 and do at least 100 trials (1000 is better) at various value of p near p_c. Copy the data for $S(p)$ and $P_\infty(p)$, and make a log-log plot of $S(p)$ and $P_\infty(p)$ versus $p - p_c$. There should be a region of your plot that is linear, indicating a possible power law. We will estimate the critical exponents β and γ in Problem 9.10. □

Problem 9.10. Finite size scaling

A better way to estimate the values of the critical exponents β and γ than fitting the p-dependence of P_∞ and $S(p)$ to their power law forms (9.50) and (9.57) near p_c is to use *finite size scaling* as we did for the Ising model in Problem 5.41 (see page 291). The underlying assumption of finite size scaling is that there is only one important length in the system near $p = p_c$, the connectedness length ξ. We write $\xi \sim |p - p_c|^{-\nu}$ and $|p - p_c| \sim \xi^{-1/\nu}$. Hence $P_\infty \sim (p - p_c)^\beta \sim \xi^{-\beta/\nu}$. For a finite system we replace ξ by L and write $P_\infty \sim L^{-\beta/\nu}$. Similar reasoning gives $S \sim L^{\gamma/\nu}$. Use program `Percolation` to generate configurations at $p = p_c$ for $L = 10$, 20, 40, 80, and 160, and determine the ratios β/ν and γ/ν. Use the exact result $\nu = 4/3$, and compare your results with the exact results for β and γ given in Table 9.2. (Because β is small, your results for β/ν are likely to not be very accurate.) □

The values of the percolation threshold p_c depend on the symmetry of the lattice and are summarized in Table 9.3. A summary of the values of the various critical exponents is given in Table 9.2. For two dimensions the static exponents are known exactly. For three dimensions no exact results are known, and the exponents have been estimated using various approximate theoretical methods and simulations. The accuracy of the numerical values for the critical exponents is consistent with the assumption of universality, which implies that the exponents are independent of the symmetry of the lattice and depend only on d.

Problem 9.11. Scaling relations for percolation

The critical exponents for percolation satisfy the same scaling relations as do thermal systems (see Table 9.1). For example, $2\beta + \gamma = d\nu$ for both thermal and systems and percolation. Use the results in Table 9.2 to confirm that the scaling relations in Table 9.1 also hold for percolation. □

9.4 Renormalization Group method for Percolation

The important idea that is incorporated into the renormalization group method is that all length scales are present at the critical point. Because all length scales are present at the percolation threshold and at the critical point for thermal systems, these systems look the same on any length scale. This property is called *self-similarity*. The mathematical expression of this property for percolation is that n_s behaves as a power law at $p = p_c$, that is, $n_s \sim s^{-\tau}$. In contrast, n_s does not exhibit power law scaling for $p \neq p_c$, and all length scales are not present.

The presence of all length scales makes the usual types of analysis not feasible because all sizes are equally important. For example, we cannot apply perturbation theory which assumes that there is something that can be neglected. The renormalization group method makes a virtue out of necessity and exploits the presence of all length scales. Because the system is self-similar, we can zoom out and expect to see the same picture. In other words, we can study the system at large length scales and find the same power law. Hence, we can ignore the details at small length scales. The renormalization group method averages over smaller length scales and determines how the system is transformed onto itself. We first consider the application of the renormalization group method to percolation to make this procedure more explicit.

The averaging over smaller length scales should be done so that it preserves the essential physics. For percolation the essential physics is connectivity. Consider a $L \times L$ square lattice and divide it into $b \times b$ cells each with b^2 sites. We adopt the rule that a cell is replaced by a single *coarse grained* occupied site if the cell spans, and is replaced by an unoccupied site if it does not. It is not clear which spanning rule to adopt, for example, vertical spanning, horizontal spanning, vertical and horizontal spanning, and vertical or horizontal spanning. We will adopt horizontal and vertical spanning because it makes enumerating the spanning clusters easier. For very large cells the different spanning rules will yield results for p_c and the critical exponents that converge to the same value.

Program `RGPercolation` implements this spanning rule and shows the original lattice and the lattice found after each coarse grained transformation. The result of these successive transformations is explored in Problem 9.12.

Problem 9.12. Visual Coarse Graining

Use `RGPercolationApp` to estimate the value of the percolation threshold. For example, confirm that for $p = 0.4$, the coarse grained lattices almost always reduce to an unoccupied site. What happens for $p = 0.8$? How can you use the properties of the coarse grained lattices to estimate p_c? □

Suppose that we make the (drastic) approximation that the occupancy of each cell is independent of all the other cells and is characterized only by the probability p' that a cell is occupied. If

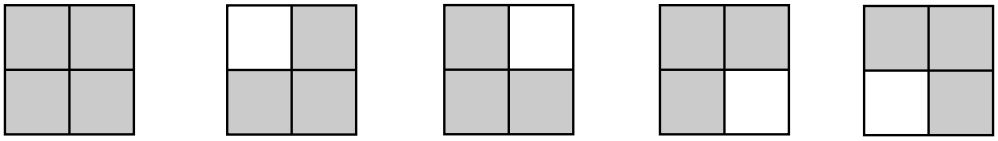

Figure 9.5: The five spanning configurations for a 2×2 cell on a square lattice. We have assumed that a cluster spans a cell only if the cluster connects the top and bottom and the left and right edges of the cell.

the sites are occupied with probability p, then the cells are occupied with probability p', where p' is given by a renormalization transformation of the form

$$p' = R(p). \tag{9.62}$$

$R(p)$ is the total probability that the sites form a spanning path.

In Figure 9.5 we show the five vertically and horizontally spanning configurations for a $b = 2$ cell. The probability p' that the cell and hence the renormalized site is occupied is given by the sum of the probabilities of all the spanning configurations:

$$p' = R(p) = p^4 + 4p^3(1-p). \tag{9.63}$$

Usually the probability p' that the renormalized site is occupied is different than the occupation probability p of the original sites. For example, suppose that we begin with $p = p_0 = 0.5$. After a single renormalization transformation, the value of p obtained from (9.63) is $p_1 = R(p_0 = 0.5) = 0.3125$. A second renormalization transformation yields $p_2 = R(p_1) = 0.0934$. It is easy to see that further transformations will drive the system to the *trivial fixed point* $p^* = 0$. Similarly, if we begin with $p = p_0 = 0.8$, we find that successive transformations drive the system to the trivial fixed point $p^* = 1$. This behavior is associated with the fact the connectedness length of the system is finite for $p \neq p_c$ and hence the change of length scale makes the connectedness length smaller after each transformation.

To find the nontrivial fixed point p^* associated with the critical threshold p_c, we need to find the special value of $p = p^*$ such that

$$p^* = R(p^*). \tag{9.64}$$

The solution of the recursion relation (9.63) for p^* yields the two trivial fixed points, $p^* = 0$ and $p^* = 1$, and the nontrivial fixed point $p^* = 0.7676$ which we associate with p_c. This value of p^* for a 2×2 cell should be compared with the best known estimate $p_c = 0.5927$ for the square lattice. Note that p^* is an example of an *unstable* fixed point because the iteration of (9.63) for p arbitrarily close but not equal to p^* will drive p to one of the two stable fixed points. The behavior of the successive transformations is summarized by the flow diagram in Figure 9.6. We see that we can associate the unstable fixed point with the percolation threshold p_c.

To calculate the critical exponent ν from the renormalization transformation $R(p)$ we note that all lengths are reduced by a factor of b on the renormalized lattice in comparison to all lengths on the original lattice. Hence ξ', the connectedness length on the renormalized lattice, is related to ξ, the connectedness length on the original lattice, by

$$\xi' = \frac{\xi}{b}. \tag{9.65}$$

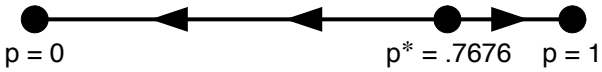

Figure 9.6: The renormalization group flow diagram for percolation on a square lattice corresponding to the recursion relation (9.63).

Because $\xi(p) = \text{constant}|p - p_c|^{-\nu}$ for $p \sim p_c$ and p_c corresponds to p^*, we have

$$|p' - p^*|^{-\nu} = \frac{1}{b}|p - p^*|^{-\nu}. \tag{9.66}$$

To find the relation between p' and p near p_c we expand $R(p)$ in (9.62) about $p = p^*$ and obtain to first order in $p - p^*$,

$$p' - p^* = R(p) - R(p^*) \approx \lambda\,(p - p^*), \tag{9.67}$$

where

$$\lambda = \left.\frac{dR}{dp}\right|_{p=p^*}. \tag{9.68}$$

We need to do a little algebra to obtain an explicit expression for ν. We first raise the left and right sides of (9.67) to the $-\nu$ power and write

$$|p' - p^*|^{-\nu} = \lambda^{-\nu}|p - p^*|^{-\nu}. \tag{9.69}$$

We compare (9.66) and (9.69) and obtain

$$\lambda^{-\nu} = b^{-1}. \tag{9.70}$$

Finally, we take the logarithm of both sides of (9.70) and obtain the desired relation for the critical exponent ν:

$$\nu = \frac{\ln b}{\ln \lambda}. \tag{9.71}$$

As an example, we calculate ν for $b = 2$ using (9.63) for $R(p)$. We write $R(p) = p^4 + 4p^3(1-p) = -3p^4 + 4p^3$ and find[5]

$$\lambda = \left.\frac{dR}{dp}\right|_{p=p^*} = \left.12p^2(1-p)\right|_{p=0.7676} = 1.6432. \tag{9.72}$$

We then use the relation (9.71) to obtain

$$\nu = \frac{\ln 2}{\ln 1.6432} = 1.40. \tag{9.73}$$

The agreement of the result (9.73) with the exact result $\nu = 4/3$ in $d = 2$ is remarkable given the simplicity of our calculation. In comparison, what would we be able to conclude if we were to measure $\xi(p)$ directly on a 2×2 lattice? This agreement is fortuitous because the accuracy of our calculation of ν is not known *a priori*.

What is the nature of the approximations that we have made in calculating ν and p_c? The basic approximation is that the occupancy of each cell is independent of all other cells. This

[5]The fact that $\lambda > 1$ implies that the fixed point is unstable.

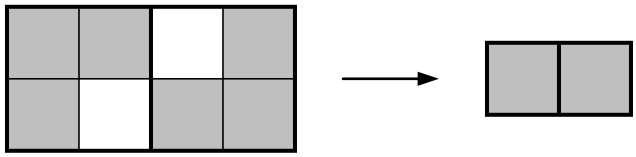

Figure 9.7: Example of an error after one renormalization. The two cells formed by sites on the original lattice on the left are not connected, but the renormalized sites on the right are connected.

assumption is correct for the original sites, but after one renormalization, we lose some of the original connecting paths and gain connecting paths that were not present in the original lattice. An example of this problem is shown in Figure 9.7. Because this surface effect becomes less important with increasing cell size, one way to improve a renormalization group calculation is to consider larger cells. A better way to obtain more accurate results is discussed in Problem 9.16.

Problem 9.13. Vertical spanning rule

Assume that a cell spans if there is a vertically spanning cluster. Choose $b = 2$ and show that $R(p) = 2p^2(1-p)^2 + 4p^3(1-p)^3 + p^4$. Find the corresponding nontrivial fixed point and the exponent ν. □

Problem 9.14. Renormalization transformation on a hexagonal lattice

(a) What are the four spanning configurations for the smallest possible cell ($b = \sqrt{3}$) on a hexagonal lattice? For this geometry the minimum cell contains three sites, at least two of which must be occupied. (See Figure 5.11 for the geometry of a hexagonal lattice.)

(b) Show that the corresponding recursion relation can be expressed as $R(p) = 3p^2 - 2p^3$. Find p^* and ν. The result $p^* = 1/2$ is exact for a hexagonal lattice. □

Problem 9.15. Renormalization transformation with $b = 3$

(a) Enumerate all the possible spanning configurations for a $b = 3$ cell on a square lattice. Assume that a cell is occupied if a cluster spans the cell vertically and horizontally. Determine the probability of each configuration and find the renormalization transformation $R(p)$.

(b) Solve for the nontrivial fixed point p^* and the critical exponent ν. One way to determnine the fixed point is by trial and error using a calculator or computer. Another straightforward way is to plot the difference $R(p) - p$ versus p and find the value of p at which $R(p) - p$ crosses the horizontal axis.[6] Are your results for p_c and ν closer to their known values than for $b = 2$? □

[6] A more sophisticated way to find the fixed point is to use a numerical method such as the Newton-Raphson method.

Problem 9.16. Cell to cell renormalization

Instead of renormalizing the set of all spanning 3×3 cells to a single occupied site as in Problem 9.15, it is better to go from cells of linear dimension $b_1 = 3$ to cells of linear dimension $b_2 = 2$. Use the fact that the connectedness lengths of the two lattices are related by $\xi(p_2)/\xi(p_1) = (b_1/b_2)^{-1}$ to derive the relation

$$\nu = \frac{\ln b_1/b_2}{\ln \lambda_1/\lambda_2}, \tag{9.74}$$

where $\lambda_i = dR(p^*, b_i)/dp$ is evaluated at the solution p^* of the fixed point equation, $R_2(b_2, p^*) = R_3(b_1, p^*)$. This "cell-to-cell" transformation yields better results in the limit in which the change in length scale is infinitesimal and is more accurate than considering large cells and renormalizing to a single site. A renormalization transformation with $b_1 = 5$ and $b_2 = 4$ gives results that are close to the exact result $\nu = 4/3$. □

9.5 The Renormalization Group Method and the One-Dimensional Ising Model

In a manner similar to our application of the renormalization group method to percolation, we will average groups of spins and then determine which parameters characterize the renormalized lattice. The result of such a calculation will be the identification of the fixed points. An unstable fixed point corresponds to a critical point. The rate of change of the renormalized parameters near a critical point yields approximate values of the critical exponents.

Although the one-dimensional Ising model does not have a critical point for $T > 0$, the application of the renormalization group method to the one-dimensional Ising model serves as a good introduction to the method (see Maris and Kadanoff).

The energy of the Ising chain with toroidal boundary conditions is (see (5.66))

$$E = -J\sum_{i=1}^{N} s_i s_{i+1} - \frac{1}{2}H\sum_{i=1}^{N}(s_i + s_{i+1}). \tag{9.75}$$

It is convenient to absorb the factors of β and define the dimensionless parameters $K = \beta J$ and $h = \beta H$. The partition function can be written as

$$Z = \sum_{\{s\}} \exp\Big[\sum_{i=1}^{N}\big(K s_i s_{i+1} + \frac{1}{2}h(s_i + s_{i+1})\big)\Big], \tag{9.76}$$

where the sum is over all possible spin configurations. We first consider $h = 0$.

We have seen that one way to obtain a renormalized lattice is to group sites or spins into cells. Another way to reduce the number of spins is to average or sum over the spins. This method of reducing the degrees of freedom is called *decimation*. For example, for the $d = 1$ Ising model we can write Z as

$$Z(K, N) = \sum_{s_1, s_2, s_3, s_4, \ldots} e^{K(s_1 s_2 + s_2 s_3)} e^{K(s_3 s_4 + s_4 s_5)\cdots}. \tag{9.77}$$

The form of (9.77) suggests that we sum over even spins s_2, s_4, ..., and write

$$Z(K,N) = \sum_{s_1,s_3,s_5\ldots} \left[e^{K(s_1+s_3)} + e^{-K(s_1+s_3)}\right]\left[e^{K(s_3+s_5)} + e^{-K(s_3+s_5)}\right]\cdots \tag{9.78}$$

We next try to write the partition function in (9.78) in its original form with $N/2$ spins and a different interaction K'. If such a rescaling were possible, we could obtain a recursion relation for K' in terms of K. We require that

$$e^{K(s_1+s_3)} + e^{-K(s_1+s_3)} = A(K)\, e^{K' s_1 s_3}, \tag{9.79}$$

where the function $A(K)$ does not depend on s_1 or s_3. If the relation (9.79) exists, we can write

$$Z(K,N) = \sum_{s_1,s_3,s_5\ldots} A(K)\, e^{K' s_1 s_3} A(K)\, e^{K' s_3 s_5}\ldots, \tag{9.80a}$$

$$= [A(K)]^{N/2} Z(K', N/2). \tag{9.80b}$$

In the limit $N \to \infty$ we know that $\ln Z$ is proportional to N, that is,

$$\ln Z = N g(K), \tag{9.81}$$

where $g(K)$ is independent of N. From (9.80b) and (9.81) we obtain

$$\ln Z(K,N) = N g(K) = \frac{N}{2}\ln A(K) + \ln Z(K', N/2) \tag{9.82a}$$

$$= \frac{N}{2}\ln A(K) + \frac{N}{2} g(K'), \tag{9.82b}$$

and

$$g(K') = 2g(K) - \ln A(K). \tag{9.83}$$

We can find the form of $A(K)$ from (9.79). We use the fact that (9.79) holds for all values of s_1 and s_3, and first consider $s_1 = s_3 = 1$ and $s_1 = s_3 = -1$ for which

$$e^{2K} + e^{-2K} = A\, e^{K'}. \tag{9.84}$$

We next consider $s_1 = 1$ and $s_3 = -1$ or $s_1 = -1$ and $s_3 = 1$ and find

$$2 = A\, e^{-K'}. \tag{9.85}$$

From (9.85) we have $A = 2e^{K'}$, and hence from (9.84) we obtain

$$e^{2K} + e^{-2K} = 2e^{2K'}, \tag{9.86}$$

or

$$K' = R(K) = \frac{1}{2}\ln\left[\cosh(2K)\right]. \qquad \text{(recursion relation)} \tag{9.87}$$

From (9.85) we find that $A(K)$ is given by

$$A(K) = 2\cosh^{1/2}(2K). \tag{9.88}$$

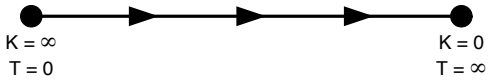

Figure 9.8: The renormalization group flow diagram for the one-dimensional Ising model in zero magnetic field.

We can use the form of $A(K)$ in (9.88) to rewrite (9.83) as

$$g(K') = 2g(K) - \ln[2\cosh^{1/2}(2K)]. \tag{9.89}$$

Equations (9.87) and (9.89) are the main results of the renormalization group analysis.

Because $\frac{1}{2}\ln\cosh(2K) \leq K$, the successive use of (9.87) leads to smaller values of K (higher temperatures) and hence smaller values of the correlation length. Thus $K = 0$ or $T = \infty$ is a trivial fixed point (see Figure 9.8). This behavior is to be expected because the Ising chain does not have a phase transition at nonzero temperature. For example, suppose we start with $K = 10$ corresponding to a low temperature. The first iteration of (9.87) gives $K' = 9.65$ and further iterations lead to $K' = 0$. Because any choice of $K \neq 0$ ultimately renormalizes to $K = 0$, we conclude that every point for $K > 0$ is in the same phase. Only at exactly zero temperature is this statement not true. Hence, there are two fixed points; the one at $T = 0$ ($K = \infty$) is unstable because any perturbation away from $T = 0$ is amplified. The fixed point at $T = \infty$ is stable. The renormalization group flows go from the unstable fixed point to the stable fixed point as shown in Figure 9.8.

Because there is no nontrivial fixed point of (9.87) between $T = 0$ and $T = \infty$, the recursion relation is reversible,[7] and we can follow the transformation backward starting at $K \approx 0$ ($T = \infty$) and going to $K = \infty$ ($T = 0$). The advantage of starting from $T \approx \infty$ is that we can start with the exact solution for $K = 0$ and iterate the recursion relation to higher values of K for which the interaction between the spins becomes increasingly important. To find the recursion relation that works in this direction we solve (9.87) for K in terms of K'. Similarly, we solve (9.89) to find $g(K)$ in terms of $g(K')$. The result is

$$K = \frac{1}{2}\cosh^{-1}(e^{2K'}), \tag{9.90}$$

$$g(K) = \frac{1}{2}\ln 2 + \frac{1}{2}K' + \frac{1}{2}g(K'). \tag{9.91}$$

Suppose we begin with $K' = 0.01$. Because this value of K' is close to zero, the effect of the spin-spin interactions is very small, and we can take $Z(K' = 0.01, N) \approx Z(K' = 0, N) = 2^N$ (all states have equal weight at high temperatures). From (9.81) we have

$$g(K' = 0.01) \approx \ln 2 \approx 0.693147. \tag{9.92}$$

[7] As we found for percolation and will find for the two-dimensional Ising model in Section 9.6, the usual renormalization transformation does not have an inverse because the number of variables decreases after each renormalization transformation, and the renormalization group is really a *semigroup*. Thus it is more accurate to refer to a renormalization group analysis or to a renormalization group method. However, it is common to refer simply to the renormalization group.

K'	K	$g(K')$	$g(K)$
0.01	0.100334	0.693147	0.698147
0.100334	0.327447	0.698147	0.745814

Table 9.4: The results of the first two iterations of the calculation of $g(K)$ for the one-dimensional Ising model from the recursion relations (9.90) and (9.91). The function $g(K)$ is related to the partition function Z by $\ln Z = Ng$ (see (9.81)).

Given $K' = 0.01$, we obtain $K = 0.100334$ from (9.90). The value of $g(K)$ for this value of K is found from (9.91) to be 0.698147. This calculation of $g(K)$ and K is the first step in an iterative procedure that can be repeated indefinitely with K' and $g(K')$ chosen to be the value of K and $g(K)$, respectively, from the previous iteration. The first two iterations are summarized in Table 9.4.

Problem 9.17. Calculation of $g(K)$

(a) Extend the calculation of $g(k)$ in Table 9.4 to larger values of K by doing several more iterations of (9.90) and (9.91). Also calculate the exact value of the free energy for the calculated values of K using (5.39) and compare your results to $g(K)$.

(b) Because the recursion relations (9.90) and (9.91) are exact, the only source of error is the first value of g. Does the error increase or decrease as the calculation proceeds? □

*__Problem 9.18.__ The recursion relations for nonzero magnetic field

(a) For nonzero magnetic field show that the function $A(K,h)$ satisfies the relation:

$$2e^{h(s_1+s_3)/2}\cosh[K(s_1+s_3)+h] = A(K,h)\,e^{K's_1s_3+\frac{1}{2}h'(s_1+s_3)}, \tag{9.93}$$

(b) Show that the recursion relations for nonzero magnetic field are

$$K' = \frac{1}{4}\ln\frac{\cosh(2K+h)\cosh(2K-h)}{\cosh^2 h}, \tag{9.94a}$$

$$h' = h + \frac{1}{2}\ln\Big[\frac{\cosh(2K+h)}{\cosh(2K-h)}\Big], \tag{9.94b}$$

and

$$\ln A(K,h) = \frac{1}{4}\ln\big[16\cosh(2K+h)\cosh(2K-h)\cosh^2 h\big]. \tag{9.94c}$$

(c) Show that the recursion relations (9.94) have a line of trivial fixed points satisfying $K^* = 0$ and arbitrary h^*, corresponding to the paramagnetic phase, and an unstable ferromagnetic fixed point at $K^* = \infty, h^* = 0$.

(d) Justify the relation

$$Z(K,h,N) = A(K,h)^{N/2}Z(K',h',N/2). \tag{9.95}$$

□

*__Problem 9.19.__ Transfer matrix method

As shown in Section 5.5.4 the partition function for the N-spin Ising chain can be written as the trace of the Nth power of the transfer matrix $\mathbf{T}$. Another way to reduce the number of degrees of freedom is to describe the system in terms of two-spin cells. We write Z as

$$Z = \mathrm{Tr}\,\mathbf{T}^N = \mathrm{Tr}\,(\mathbf{T}^2)^{N/2} = \mathrm{Tr}\,\mathbf{T}'^{N/2}. \tag{9.96}$$

The transfer matrix for two-spin cells, $\mathbf{T}^2$, can be written as

$$\mathbf{T}^2 = \mathbf{T}\mathbf{T} = \begin{pmatrix} e^{2K+2h} + e^{-2K} & e^{h} + e^{-h} \\ e^{-h} + e^{h} & e^{2K-2h} + e^{-2K} \end{pmatrix}. \tag{9.97}$$

We require that $\mathbf{T}'$ have the same form as $\mathbf{T}$:

$$\mathbf{T}' = C \begin{pmatrix} e^{K'+h'} & e^{-K'} \\ e^{-K'} & e^{K'-h'} \end{pmatrix}. \tag{9.98}$$

A parameter C must be introduced because matching (9.97) with (9.98) requires matching three matrix elements, which is impossible with only two variables, K' and h'.

(a) Show that the three unknowns satisfy the three conditions:

$$Ce^{K'}e^{h'} = e^{2K+2h} + e^{-2K} \tag{9.99a}$$

$$Ce^{-K'} = e^{h} + e^{-h} \tag{9.99b}$$

$$Ce^{K'}e^{-h'} = e^{2K-2h} + e^{-2K}. \tag{9.99c}$$

(b) Show that the solution of (9.99) can be written as

$$e^{-2h'} = \frac{e^{2K-2h} + e^{-2K}}{e^{2K+2h} + e^{-2K}} \tag{9.100a}$$

$$e^{-4K'} = \frac{e^{4K} + e^{-2h} + e^{-2h} + e^{4K}}{(e^{h} + e^{-h})^2} \tag{9.100b}$$

$$C^4 = [e^{4K} + e^{-2h} + e^{-2h} + e^{4K}][e^{h} + e^{-h}]^2. \tag{9.100c}$$

(c) Show that the recursion relations in (9.100) reduce to (9.87) for $h = 0$. For $h \neq 0$ start from some initial state K_0, H_0 and calculate a typical renormalization group trajectory. To what phase (paramagnetic or ferromagnetic) does the fixed point correspond? □

9.6 *The Renormalization Group Method and the Two-Dimensional Ising Model

As pointed out by Wilson,[8] there is no recipe for constructing a renormalization group transformation, and we will consider only one possible approach. In particular, we consider the majority

[8] Ken Wilson was awarded the 1982 Nobel Prize in Physics for developing the renormalization group method for critical phenomena.

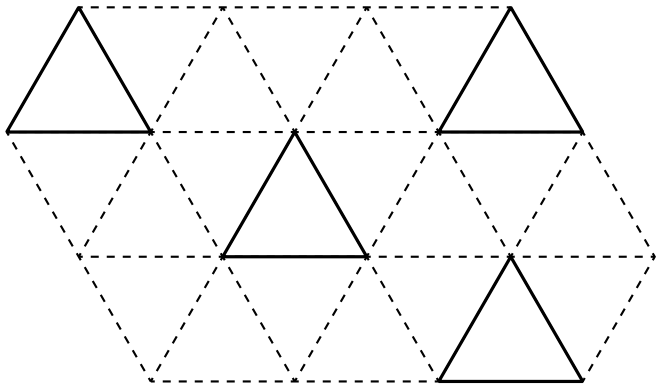

Figure 9.9: Cell spins on a hexagonal lattice. The solid lines indicate intracell interactions; the dotted lines show the intercell interactions.

rule transformation developed by Niemeijer and van Leeuwen for the ferromagnetic Ising model on a hexagonal lattice.

The idea of their method is to divide the original lattice with lattice spacing a into cells as we did for percolation in Section 9.4, and replace the original site spins $s_i = \pm 1$ by the renormalized cell spins $\mu_\alpha = \pm 1$. The Latin indices i and j denote the original lattice sites, and the Greek indices α and β denote the renormalized cell spins. As shown in Figure 9.9 we will group the sites of the original hexagonal lattice into cells of three sites each. The cells also form a hexagonal lattice with the lattice constant $a' = \sqrt{3}a$, so that the length rescaling parameter is $b = \sqrt{3}$. We suggest that you focus on the ideas involved in the following calculation rather than the details.

It is convenient to write the energy of the spins in the form[9]

$$\widetilde{E} = \beta E = -K \sum_{\langle ij \rangle} s_i s_j, \tag{9.101}$$

and the partition function as

$$Z(K) = \sum_{\{s\}} e^{-\widetilde{E}(\{s\})}. \tag{9.102}$$

We have incorporated the factor of β into the energy and have introduced the notation $\widetilde{E} = \beta E$. For simplicity, we will consider $h = 0$ so that there is only one coupling constant $K = \beta J$.

The energy of the renormalized lattice can be written as

$$\widetilde{E}' = \widetilde{E}_0 + \widetilde{V}, \tag{9.103}$$

where $\widetilde{E}_0$ represents the sum of all the interactions between spins within the same cell, and $\widetilde{V}$ is the interaction of spins between different cells. We write

$$\widetilde{E}_0 = -K \sum_{\alpha} \sum_{i,j \subset \alpha} s_i s_j, \tag{9.104}$$

[9]More advanced readers will recognize that E should be replaced by the Hamiltonian.

where the sum over α represents the sum over all cells. The spins in cell α satisfy the condition $\mu_\alpha = \text{sgn}(\sum_{i=1}^{3} s_{i,\alpha})$ (the majority rule). The energy of cell α has the form

$$\widetilde{E}_{0,\alpha} = -K(s_{1,\alpha}s_{2,\alpha} + s_{1,\alpha}s_{3,\alpha} + s_{2,\alpha}s_{3,\alpha}). \tag{9.105}$$

We write the interaction $\widetilde{V}$ as

$$\widetilde{V} = -K \sum_{\substack{\alpha,\beta \\ \alpha\neq\beta}} \sum_{i\subset\alpha} \sum_{j\subset\beta} s_i s_j. \tag{9.106}$$

The representation (9.103)–(9.106) is exact.

The replacement of the original site spins by cell spins leads to an energy that does not have the same form as (9.101). That is, the new energy involves interactions between cell spins that are not nearest neighbors. Nevertheless, we will assume that the new energy has the same form:

$$\widetilde{G} + \widetilde{E}' = -K' \sum_{\langle\alpha\beta\rangle} \mu_\alpha \mu_\beta. \tag{9.107}$$

The term $\widetilde{G}$ in (9.107) is independent of the cell spin configurations, and the sum on the right-hand side is over nearest-neighbor cells.

The goal is to obtain a recursion relation

$$K' = R(K), \tag{9.108}$$

and a nontrivial fixed point K^* such that

$$\lambda_K = \left.\frac{\partial K'}{\partial K}\right|_{K=K^*}, \tag{9.109}$$

and

$$\nu = \frac{\ln \lambda_K}{\ln b}, \tag{9.110}$$

where b is the length rescaling parameter.

In the following we will treat the interactions of the spins within the cells exactly and the interactions between the cells approximately. The renormalized energy is given formally by

$$e^{-\widetilde{G}-\widetilde{E}'} = \sum_{\{s\}} P(\mu, s)\, e^{-(\widetilde{E}_0+\widetilde{V})}. \tag{9.111}$$

The function $P(\mu, s)$ transforms the original three spins to the cell spin and implements the majority rule so that the cell spin equals the sign of the sum of the site spins in the cell. We can write $P(\mu, s)$ for cell spin α as

$$P(\mu_\alpha, s) = \delta\big(\mu_\alpha - \text{sgn}(s_1 + s_2 + s_3)\big). \tag{9.112}$$

It is convenient to treat the noninteracting cells as a reference system (see Section 8.6) and treat the interaction between the cell spins approximately. We can show that[10]

$$e^{-\widetilde{G}} e^{-\widetilde{E}'} = Z_0 \big\langle e^{-\widetilde{V}} \big\rangle_0. \tag{9.115}$$

[10] We write the average of an arbitrary function $A(s)$ over the noninteracting cells as

$$\langle A \rangle_0 = \frac{\sum_{\{s\}} A(s)\, P(\mu, s)\, e^{-\widetilde{E}_0(s)}}{\sum_{\{s\}} P(\mu, s)\, e^{-\widetilde{E}_0(s)}}. \tag{9.113}$$

where the average is over the original spin variables with respect to $\widetilde{E}_0$, $Z_0 = z(\mu)^{N'}$, $N' = N/b^d$ is the number of cells in the renormalized lattice, and $z(\mu)$ is the sum over the internal spin states of one cell for a given value of μ. The average $\langle e^{-\widetilde{V}} \rangle_0$ is over the noninteracting cells.

We take the logarithm of both sides of (9.115) and obtain

$$\widetilde{G} + \widetilde{E}' = -N' \ln z - \ln \langle e^{-\widetilde{V}} \rangle_0. \tag{9.116}$$

We can identify

$$g = \frac{\widetilde{G}}{N} = \frac{N'}{N} \ln z = \frac{1}{b^d} \ln z, \tag{9.117}$$

and

$$\widetilde{E}' = -\ln \langle e^{-\widetilde{V}} \rangle_0. \tag{9.118}$$

Note that (9.118) has the same form as (8.8) and (8.110).

We first calculate z and g and then evaluate the average in (9.118). The sum over the spins in a given cell for $\mu = 1$ can be written as

$$z(\mu = 1) = \sum_{\{s\}} e^{K(s_1 s_2 + s_2 s_3 + s_3 s_1)}. \tag{9.119}$$

The four possible states of the three spins s_1, s_2, s_3 with the restriction that $\mu = 1$ are given in Figure 9.10. Hence,

$$z(\mu = 1) = e^{3K} + 3\, e^{-K}. \tag{9.120}$$

In the absence of a magnetic field the sum for $\mu = -1$ gives the same value for z (see Problem 9.20). From (9.117) we have

$$g(K) = \frac{1}{3} \ln(e^{3K} + 3\, e^{-K}). \tag{9.121}$$

Problem 9.20. Calculation of $z(\mu = -1)$
Calculate $z(\mu = -1)$ and show that $z(\mu)$ is independent of the sign of μ. □

The difficult part of the calculation is the evaluation of the average $\langle e^{-\widetilde{V}} \rangle_0$. We will evaluate it approximately by keeping only the first cumulant (see Section 8.4.1). Because the cumulant expansion is a power series in $K = \beta J$, it is reasonable to assume that the series converges given that $K_c \approx 0.275$ for a hexagonal lattice. We have

$$\ln \langle e^{-\widetilde{V}} \rangle_0 = \sum_{n=1}^{\infty} \frac{(-1)^n}{n!} M_n, \tag{9.122}$$

We then multiply the top and bottom of (9.111) by $Z_0 = \sum_{\{s'\}} P(\mu, s')\, e^{-\widetilde{E}_0}$, the partition function associated with $\widetilde{E}_0$:

$$e^{-\widetilde{G}} e^{-\widetilde{E}'} = \sum_{\{s\}} P(\mu, s)\, e^{-\widetilde{E}_0} \frac{\sum_{\{s'\}} P(\mu, s')\, e^{-(\widetilde{E}_0 + \widetilde{V})}}{\sum_{\{s'\}} P(\mu, s')\, e^{-\widetilde{E}_0}} \tag{9.114a}$$

$$= Z_0 \langle e^{-\widetilde{V}} \rangle_0. \tag{9.114b}$$

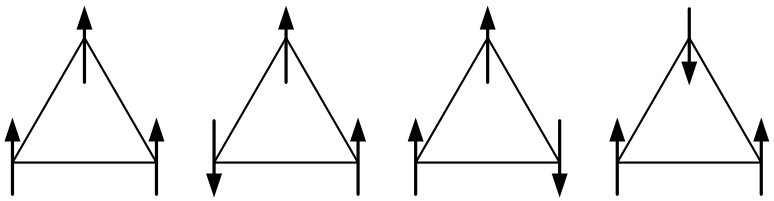

Figure 9.10: The four possible configurations of the three spin cell on a hexagonal lattice such that $\mu = 1$.

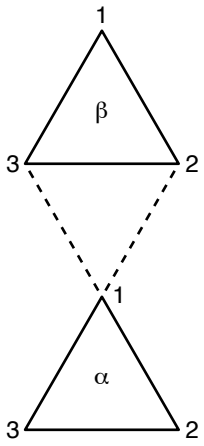

Figure 9.11: The couplings (dotted lines) between nearest-neighbor cell spins $\widetilde{V}_{\alpha\beta}$.

and keep only the first cumulant

$$M_1 = \langle \widetilde{V} \rangle_0. \tag{9.123}$$

The first approximation to the intercell interaction $\widetilde{V}$ can be written as (see Figure 9.11)

$$\widetilde{V}_{\alpha\beta} = -K s_{1,\alpha}[s_{2,\beta} + s_{3,\beta}]. \tag{9.124}$$

Note that $\widetilde{V}$ in (9.124) includes only the interaction of two nearest neighbor cells, and this approximation does not preserve the symmetry of a hexagonal lattice. However, this approximation is consistent with our assumption that the renormalized energy has the same form as the original energy. Because $\widetilde{E}_0$ does not couple different cells, we have

$$\langle \widetilde{V}_{\alpha\beta} \rangle_0 = -2K \langle s_{1,\alpha} s_{2,\beta} \rangle_0 = -2K \langle s_{1,\alpha} \rangle_0 \langle s_{2,\beta} \rangle_0. \tag{9.125}$$

The factor of 2 in (9.125) arises from the fact that $\langle s_{2,\beta} \rangle = \langle s_{3,\beta} \rangle$.

From (9.125) we see that we need to find $\langle s_{1,\alpha} \rangle_0$. Suppose that $\mu_\alpha = 1$. The four states

consistent with this condition are shown in Figure 9.10. It is easy to see that

$$\langle s_{1,\alpha}\rangle_0 = \frac{1}{z}\sum_{\{s\}} s_1 e^{K(s_1s_2+s_2s_3+s_3s_1)} \tag{9.126a}$$

$$= \frac{1}{z}\big[+1e^{3K}+1e^{-K}+1e^{-K}-1e^{-K}\big] \tag{9.126b}$$

$$= \frac{1}{z}[e^{3K}+e^{-K}]. \qquad (\mu_\alpha = +1). \tag{9.126c}$$

Similarly, we can show that

$$\langle s_{1,\alpha}\rangle_0 = \frac{1}{z}[-e^{3K}-e^{-K}] = -\frac{1}{z}[e^{3K}+e^{-K}] \qquad (\mu_\alpha = -1) \tag{9.126d}$$

Hence, we have

$$\langle s_{1,\alpha}\rangle_0 = \frac{1}{z}[e^{3K}+e^{-K}]\mu_\alpha. \tag{9.127}$$

From (9.125) and (9.127) we have

$$\langle \widetilde{V}_{\alpha\beta}\rangle_0 = -2Kf(K)^2\mu_\alpha\mu_\beta, \tag{9.128}$$

where

$$f(K) = \frac{e^{3K}+e^{-K}}{e^{3K}+3e^{-K}}. \tag{9.129}$$

Hence,

$$\langle \widetilde{V}\rangle_0 = \sum_{\langle\alpha\beta\rangle}\langle \widetilde{V}_{\alpha\beta}\rangle_0 = -2Kf(K)^2\sum_{\langle\alpha\beta\rangle}\mu_\alpha\mu_\beta \tag{9.130a}$$

$$= -K'\sum_{\langle\alpha\beta\rangle}\mu_\alpha\mu_\beta. \tag{9.130b}$$

Note that $\langle\widetilde{V}\rangle_0$ has the same form as the original nearest neighbor interaction with a renormalized value of the interaction. If we compare (9.128) and (9.130b), we find the recursion relation

$$K' = R(K) = 2Kf(K)^2, \tag{9.131}$$

and

$$\widetilde{E}' = -K'\sum_{\langle\alpha\beta\rangle}\mu_\alpha\mu_\beta. \tag{9.132}$$

Because $f(K=0) = 1/2$ and $f(K=\infty) = 1$, it is easy to see that there are trivial fixed points at $K^* = 0$ and $K^* = \infty$. The nontrivial fixed point occurs at $f(K) = 1/\sqrt{2}$ or at

$$K^* = \frac{1}{4}\ln(2\sqrt{2}+1) \approx 0.3356. \tag{9.133}$$

The exact answer for K_c for a hexagonal lattice is $K_c = \frac{1}{3}\ln 3 = 0.2747$. We also have

$$\lambda_K = \frac{dK}{dK}\Big|_{K=K^*} = 1.624, \tag{9.134}$$

and hence

$$\nu = \frac{\ln 1.624}{\ln \sqrt{3}} \approx 0.882. \tag{9.135}$$

For comparison, the exact result is $\nu = 1$ (see Table 5.1).

Problem 9.21. Confirm the above results for K^*, λ_K, and ν. □

We can extend the renormalization group analysis by considering higher order cumulants. The second order cumulant introduces two new interactions that are not in the original energy. That is, the cell spins interact not only with nearest-neighbor cell spins, but also with second and third neighbor cell spins. Hence, for consistency we have to include in our original energy second and third neighbor interactions also. Good results can usually be found by stopping at the second cumulant. More details can be found in the references.

Vocabulary

Landau and Landau-Ginzburg theory
mean-field critical exponents
Ginzburg criterion
scaling relations, universality
percolation, connectivity
cluster, spanning cluster
coarse graining, renormalization group method
recursion relation

Additional Problems

Problem 9.22. Alternate derivation of Fisher's scaling law

Another way to express the scaling hypothesis is to assume that for $h = 0$, $G(r)$ near $\epsilon = 0$ has the form

$$G(r) \sim \frac{1}{r^{d-2+\eta}}\psi_{\pm}(r/\xi), \tag{9.136}$$

where $\psi_{\pm}$ is an unspecified function that depends only on the ratio r/ξ. Use (9.136) and the relation (9.34) to obtain Fisher's scaling law, $\gamma = \nu(2-\eta)$. □

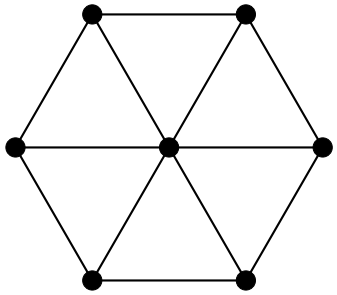

Figure 9.12: The seven site cell considered in Problem 9.24.

Problem 9.23. Percolation in one dimension

Choose a simple cell for percolation in one dimension and show that $p_c = 1$ and $\nu = 1$ exactly. □

*__Problem 9.24.__ Seven site cell for percolation

We can generalize the triangular cell considered in Problem 9.14 and consider the seven site cell shown in Figure 9.12 and assume that the cell is occupied if the majority of its sites are occupied.

(a) Show that the recursion relation is

$$p' = R(p) = 35p^4 - 84p^5 + 70p^6 - 20p^7. \tag{9.137}$$

(b) Show that (9.137) has a nontrivial fixed point at $p^* = 0.5$ and that the connectedness length exponent ν is given by

$$\nu = \frac{\ln 7}{2 \ln \frac{7}{3}} \approx 1.243. \tag{9.138}$$

□

Problem 9.25. Simulations of the two-dimensional XY (planar) model

We briefly mentioned the planar or XY model on page 444. In this model the spins are located on a d-dimensional lattice, but are restricted to point in any direction in the plane. The interaction between two nearest neighbor spins is given by $-J\mathbf{s}_1 \cdot \mathbf{s}_2$, where $\mathbf{s}_1$ and $\mathbf{s}_2$ are two unit spin vectors.

One of the interesting features of the XY model in two dimensions is that the mean magnetization $\langle M \rangle = 0$ for all nonzero temperatures, but there is a phase transition at a nonzero temperature $T_{\rm KT}$ known as the Kosterlitz-Thouless transition. For $T \leq T_{\rm KT}$ the spin-spin correlation $C(r)$ decreases as a power law; for $T > T_{\rm KT}$ C(r) decreases exponentially. The power law decay of $C(r)$ for $T \leq T_{\rm KT}$ implies that every temperature below $T_{\rm KT}$ acts as a critical point.

Program `XYModel` indexprograms!XYModel uses the Metropolis algorithm to simulate the XY model in two dimensions. In this case a spin is chosen at random and rotated by a random angle up to a maximum value δ.

(a) Rewrite the interaction $-J\mathbf{s}_i \cdot \mathbf{s}_j$ between nearest neighbor spins i and j in a simpler form by substituting $s_{i,x} = \cos\theta_i$ and $s_{i,y} = \sin\theta_i$, where the phase θ_i is measured from the horizontal axis in the counter-clockwise direction. Show that the result is $-J\cos(\theta_i - \theta_j)$.

(b) An interesting feature of the XY model is the existence of vortices and anti-vortices. A vortex is a region of the lattice where the spins rotate by at least 2π as you trace a closed path. Run the simulation with the default parameters and observe the locations of the vortices. Follow the arrows as they turn around a vortex. A vortex is indicated by a square box. What is the difference between a positive (blue) and negative (red) vortex? Does a vortex ever appear isolated? Count the number of positive vortices and negative vortices. Is the number the same at all times?

(c) Click the `Reset` button and change the temperature to 0.2. Make sure the initial configuration is set to random. You should see quenched-in vortices which don't change with time. Are there an equal number of positive and negative vortices? Are there isolated vortices whose centers are more than a lattice spacing apart?

(d) Click the `Reset` button and set the initial configuration to ordered and the temperature to 0.2. Also set steps per display to 100 so that the simulation will run much faster. Run the simulation for at least 1000 mcs and record the estimates of the specific heat and the susceptibility. Repeat for temperatures from 0.3 to 1.5 in steps of 0.1. Plot the energy and specific heat versus the temperature. Near the specific heat and susceptibility peaks take more data in temperature intervals of 0.02. Do the peaks in the susceptibility and specific heat occur (approximately) at the same temperature? Is the vorticity (the mean number density of vortices) a smooth function of the temperature?

(e) Choose a temperature which is near the peak in the susceptibility and look at configurations showing the vortices. At the peak in the susceptibility (the Kosterlitz-Thouless transition) is there any evidence that the positive vortices are moving away from the negative vortices? The Kosterlitz-Thouless transition is due to this unbinding of vortex pairs.

Suggestions for Further Reading

David Chandler, *Introduction to Modern Statistical Mechanics*, Oxford University Press (1987). See Chapter 5 for a clear explanation of the renormalization group method.

R. J. Creswick, H. A. Farach, and C. P. Poole, Jr., *Introduction to Renormalization Group Methods in Physics*, John Wiley & Sons (1992).

Alastair Bruce and David Wallace, "Critical point phenoma: Universal physics at large length scales," in *The New Physics*, edited by Paul Davies, Cambridge University Press (1989).

Cyril Domb, *The Critical Point: A Historical Introduction to the Modern Theory of Critical Phenomena*, Taylor & Francis (1996). The physics is explained at the graduate level, but much of it is accessible to undergraduates, especially the discussion of the history of various developments.

H. Gould, J. Tobochnik, and W. Christian, *An Introduction to Computer Simulation Methods*, third edition, Addison-Wesley, 2006), Chapter 12.

Kerson Huang, *Statistical Mechanics*, second edition, John Wiley & Sons (1987).

Leo P. Kadanoff, *Statistical Physics: Statics, Dynamics, and Renormalization*, World-Scientific (2000).

H. J. Maris and L. P. Kadanoff, "Teaching the renormalization group," Am. J. Phys. **46**, 652–657 (1978).

Ramit Mehr, Tal Grossman, N. Kristianpoller, and Yuval Gefen, "Simple percolation experiment in two dimensions," Am. J. Phys. **54**, 271–273 (1986).

Michael Plischke and Birger Bergersen, *Equilibrium Statistical Physics*, third edition, World Scientific (2006). An excellent graduate level text.

P. J. Reynolds, H. E. Stanley, and W. Klein, "A large cell Monte Carlo renormalization group for percolation," Phys. Rev. B **21**, 1223–1245 (1980). Our discussion of percolation in Section 9.4 is mostly based on this paper.

D. Stauffer, "Percolation clusters as teaching aid for Monte Carlo simulation and critical exponents," Am. J. Phys. **45**,1001–1002 (1977).

Dietrich Stauffer and Amnon Aharony, *Introduction to Percolation Theory*, second edition, Taylor & Francis (1992).

D. J. Wallace and R. K. P. Zia, "The renormalisation group approach to scaling in physics," Rep. Prog. Phys. **41**, 1–85 (1978).

K. G. Wilson, "Problems in physics with many scales of length," Sci. Am. **241** (8), 140–157 (1979).

Richard Zallen, *The Physics of Amorphous Solids*, John Wiley & Sons (1983). This monograph discusses applications of percolation theory.